

A Novel Two Layer Constant Power Control Of 15 DFIG Wind Turbines With Supercapacitor Energy Storage

V.Krishnamurthy ¹, Ch.Rajesh Kumar ²

¹Department of electrical and electronics engineering, Narayana Engineering College, Nellore,Ap,India.

² Asst.proffesor Department of electrical and electronics engineering, Narayana Engineering College, Nellore,Ap,India.

Abstract-Wind energy is an unpredictable and fluctuating energy source, this will creates the fluctuations in the output power. With the increasing penetration of wind power into electric power grids, energy storage devices will be required to dynamically match the intermittency of wind energy. This paper proposes a novel two-layer constant power control scheme for a wind farm equipped with doubly fed induction generator (DFIG) wind turbines. Each DFIG wind turbine is equipped with a supercapacitor energy storage system (ESS) and is controlled by the low-layer wind turbine generator (WTG) controllers and coordinated by a high-layer wind farm supervisory controller (WFSC). The WFSC generates the active power references for the low-layer WTG controllers according to the active power demand from or generation commitment to the grid operator; the low-layer WTG controllers then regulate each DFIG wind turbine to generate the desired amount of active power, where the deviations between the available wind energy input and desired active power output are compensated by the ESS. Simulation studies are carried out in MATLAB/SIMULINK on a wind farm equipped with 15 DFIG wind turbines to verify the effectiveness of the proposed control scheme.

Keywords- Constant power control (CPC), doubly fed induction generator (DFIG), energy storage, supervisory controller, wind turbine

I.INTRODUCTION

WIND TURBINE generators (WTGs) are usually controlled to generate maximum electrical power from wind under normal wind conditions. However, because of the variations of the wind speed, the generated electrical power of a WTG is usually fluctuated. Currently, wind energy only provides about 1%–2% of the U.S.'s electricity supply. At such a penetration level, it is not necessary to require WTGs to participate in automatic generation control, unit commitment, or frequency regulation. However, it is reasonable to expect that wind power will be

capable of becoming a major contributor to the nation's and world's electricity supply over the next three decades. For instance, the European Wind Energy Association has set a target to satisfy more than 22% of European electricity demand with wind power by 2030 [1]. In the U.S., according to a report [2] by the Department of Energy, it is feasible to supply 20% of the nation's electricity from wind by 2030. At such high levels of penetration, it will become necessary to require WTGs to supply a desired amount of active power to participate in automatic generation control or frequency regulation of the grid [3]. However, the intermittency of wind resources can cause high rates of change (ramps) in power generation [4], which is a critical issue for balancing power systems. Moreover, to optimize the economic performance of power systems with high penetrations of wind power, it would be desired to require WTGs to participate in unit commitment, economic dispatch, or electricity market operation [5]. In practice, short-term wind power prediction [6] is carried out to help WTGs provide these functions. However, even using the state-of-the-art methods, prediction errors are present [5]. Under these conditions, the replacement power is supported by reserves, which, however, can be more expensive than base electricity prices [7]. To enable WTGs to effectively participate in frequency and active power regulation, unit commitment, economic dispatch, and electricity market operation, energy storage devices will be required to dynamically match the intermittency of wind energy. In [8], the authors investigated and compared different feasible electric energy storage technologies for intermittent renewable energy generation, such as wind power. Currently, pumped water and compressed air are the most commonly used energy storage technologies for power grids due to their low capital costs [9]. However, these two technologies are heavily dependent on geographical location with relatively low round-trip efficiency. Compared with their peers, batteries and supercapacitors are more efficient, have a quicker

the dc bus of the DFIG converters during transients, thereby enhancing the low-voltage ride through capability of the WTG [10].

III. CONTROL OF INDIVIDUAL DFIG WIND TURBINE

The control system of each individual DFIG wind turbine generally consists of two parts: 1) the electrical control of the DFIG and 2) the mechanical control of the wind turbine blade pitch angle [14], [15] and yaw system. Control of the DFIG is achieved by controlling the RSC, the GSC, and the ESS (see Fig. 1). The control objective of the RSC is to regulate the stator-side active power P_s and reactive power Q_s independently. The control objective of the GSC is to maintain the dc-link voltage V_{dc} constant and to regulate the reactive power Q_g that the GSC exchanges with the grid. The control objective of the ESS is to regulate the active power P_g that the GSC exchanges with the grid. In this paper, the mechanical control of the wind turbine blade pitch angle is similar to that in [15].

A. Control of the RSC

Fig. 2 shows the overall vector control scheme of the RSC, in which the independent control of the stator active power P_s and reactive power Q_s is achieved by means of rotor current regulation in a stator-flux-oriented synchronously rotating reference frame [16]. Therefore, the overall RSC control scheme consists of two cascaded control loops. The outer control loop regulates the stator active and reactive powers independently, which generates the reference signals i_{dr}^* and i_{qr}^* of the d - and q -axis current components, respectively, for the inner-loop current regulation. The outputs of the two current controllers are compensated by the corresponding cross-coupling terms v_{dr0} and v_{qr0} [14], respectively, to form the total voltage signals v_{dr} and v_{qr} . They are then used by the pulsewidth modulation (PWM) module to generate the gate control signals to drive the RSC. The reference signals of the outer-loop power controllers are generated by the high-layer WFSC.

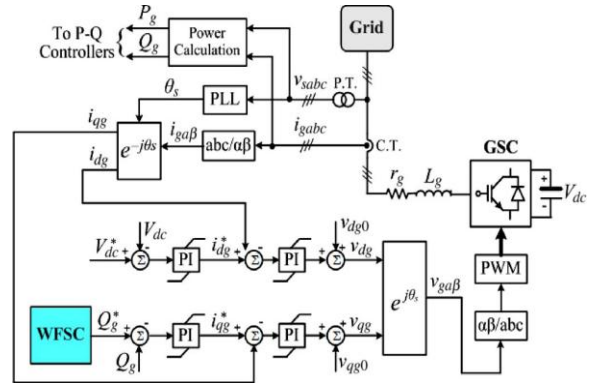


Fig.3. Overall vector control scheme of the GSC.

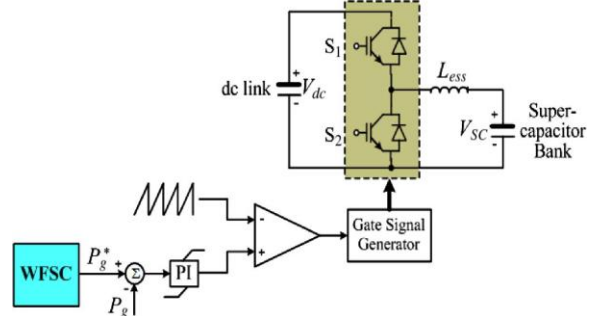


Fig.4 .Configuration and control of the ESS.

B. Control of the GSC

Fig. 3 shows the overall vector control scheme of the GSC, in which the control of the dc-link voltage V_{dc} and the reactive power Q_g exchanged between the GSC and the grid is achieved by means of current regulation in a synchronously rotating reference frame [16]. Again, the overall GSC control scheme consists of two cascaded control loops. The outer control loop regulates the dc-link voltage V_{dc} and the reactive power Q_g , respectively, which generates the reference signals i_{dg}^* and i_{qg}^* of the d - and q -axis current components, respectively, for the inner-loop current regulation. The outputs of the two current controllers are compensated by the corresponding cross-coupling terms v_{dg0} and v_{qg0} [14], respectively, to form the total voltage signals v_{dg} and v_{qg} . They are then used by the PWM module to generate the gate control signals to drive the GSC. The reference signal of the outer-loop reactive power controller is generated by the high-layer WFSC.

C. Configuration and Control of the ESS

Fig. 4 shows the configuration and control of the ESS. The ESS consists of a supercapacitor bank and a two-quadrant dc/dc converter connected to the dc link of the DFIG. The dc/dc converter contains two insulated-gate bipolar transistor (IGBT) switches S1 and S2. Their duty ratios are controlled to regulate the active power P_g that the GSC exchanges with the grid. In this configuration, the dc/dc converter can operate in two different modes, i.e., buck or boost

mode, depending on the status of the two IGBT switches. If S1 is open, the dc/dc

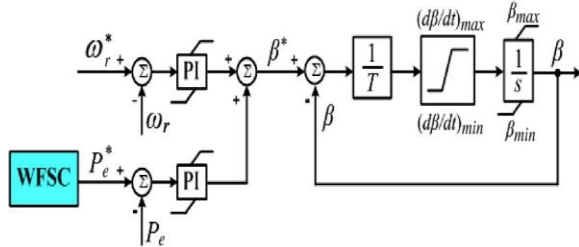


Fig.5. Blade pitch control for the wind turbine. converter operates in the boost mode; if S₂ is open, the dc/dc converter operates in the buck mode. The duty ratio D₁ of S₁ in the buck mode can be approximately expressed as

$$D_1 = \frac{V_{SC}}{V_{dc}} \quad (2)$$

and the duty ratio D₂ of S₂ in the boost mode is D₂ = 1 – D₁. In this paper, the nominal dc voltage ratio V_{SC,n}/V_{dc,n} is 0.5, where V_{SC,n} and V_{dc,n} are the nominal voltages of the supercapacitor bank and the DFIG dc link, respectively. Therefore, the nominal duty ratio D_{1,n} of S₁ is 0.5. The operating modes and duty ratios D₁ and D₂ of the dc/dc converter are controlled depending on the relationship between the active powers P_r of the RSC and P_g of the GSC. If P_r is greater than P_g, the converter is in buck mode and D₁ is controlled, such that the supercapacitor bank serves as a sink to absorb active power, which results in the increase of its voltage V_{SC}. On the contrary, if P_g is greater than P_r, the converter is in boost mode and D₂ is controlled, such that the supercapacitor bank serves as a source to supply active power, which results in the decrease of its voltage V_{SC}. Therefore, by controlling the operating modes and duty ratios of the dc/dc converter, the ESS serves as either a source or a sink of active power to control the generated active power of the WTG. In Fig. 4, the reference signal P_g^{*} is generated by the high-layer WFSC.

D. Wind Turbine Blade Pitch Control

Fig. 5 shows the blade pitch control for the wind turbine, where ω_r and P_e (= P_s + P_g) are the rotating speed and output active power of the DFIG, respectively. When the wind speed is below the rated value and the WTG is required to generate the maximum power, ω_r and P_e are set at their reference values, and the blade pitch control is deactivated. When the wind speed is below the rated value, but the WTG is required to generate a constant power less than the maximum power, the active power controller may be activated, where the reference signal P_e^{*} is generated by the high-layer WFSC and P_e takes the actual measured value. The active power controller adjusts the blade pitch angle to reduce the mechanical power that the turbine extracts from

wind. This reduces the imbalance between the turbine mechanical power and the DFIG output active power, thereby reducing the mechanical stress in the WTG and stabilizing the WTG system. Finally, when the wind speed increases above the rated value, both ω_r and P_e take the actual measured values, and both the speed and active power controllers are activated to adjust the blade pitch angle.

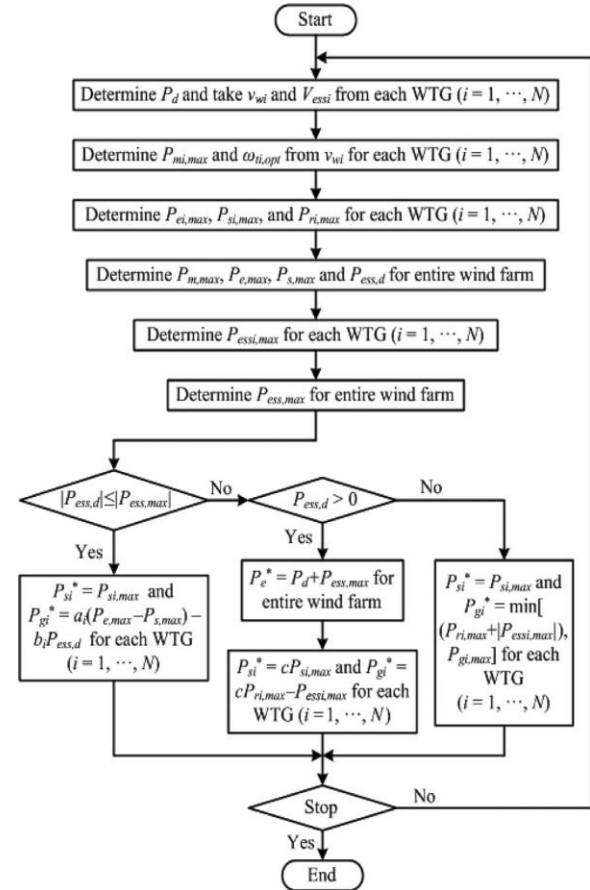


Fig.6. Flowchart of implementation of the WFSC.

IV. WIND FARM SUPERVISORY CONTROL

The objective of the WFSC is to generate the reference signals for the outer-loop power controllers of the RSC and GSC, the controller of the dc/dc converter, and the blade pitch controller of each WTG, according to the power demand from or the generation commitment to the grid operator. The implementation of the WFSC is described by the flowchart in Fig. 6, where P_d is the active power demand from or the generation commitment to the grid operator; v_{wi} and V_{ess_i} are the wind speed in meters per second and the voltage of the supercapacitor bank measured from WTG (i = 1, . . . , N), respectively; and N is the number of WTGs in the wind farm. Based on v_{wi},

rotational speed $\omega_{i,opt}$ in radians per second of the wind turbine can be determined, which is proportional to the wind speed v_{wi} at a certain pitch angle β_i

$$\omega_{ti,opt} = k(\beta_i)v_{wi} \quad (3)$$

where k is a constant at a certain value of β_i . Then, the maximum mechanical power $P_{mi,max}$ that the wind turbine extracts from the wind can be calculated by the well-known wind turbine aerodynamic characteristics

$$P_{mi,max} = \frac{1}{2} \rho_i A_r v_{wi}^3 C_{pi}(\lambda_{i,opt}, \beta_i) \quad (4)$$

where ρ_i is the air density in kilograms per cubic meter; $A_r = \pi R^2$ is the area in square meters swept by the rotor blades, with R being the blade length in meters; and C_{pi} is the power coefficient, which is a function of both tip-speed ratio λ_i and the blade pitch angle β_i , where λ_i is defined by

$$\lambda_i = \frac{\omega_{ti} R}{v_{wi}} \quad (5)$$

In (4), $\lambda_{i,opt}$ is the optimal tip-speed ratio when the wind turbine rotates with the optimal speed $\omega_{ti,opt}$ at the wind speed v_{wi} .

Given $P_{mi,max}$, the maximum active power $P_{ei,max}$ generated by the WTG can be estimated by taking into account the power losses of the WTG [14]

$$P_{ei,max} = P_{mi,max} - P_{Li} = P_{si,max} + P_{ri,max} \quad (6)$$

where P_{Li} is the total power losses of WTG i , which can be estimated by the method in [14]; $P_{si,max}$ and $P_{ri,max}$ are the maximum DFIG stator and rotor active powers of WTG i , respectively. In terms of the instantaneous variables in Fig.1, the stator active power P_s can be written in a synchronously rotating dq reference frame [16] as follows:

$$P_s = \frac{3}{2} (V_{ds} i_{ds} + V_{qs} i_{qs}) \approx \frac{3}{2} [w_s L_m (i_{qs} i_{dr} - i_{ds} i_{qr}) + r_s (i_{ds}^2 + i_{qs}^2)] \quad (7)$$

where v_{ds} and v_{qs} are the d - and q -axis voltage components of the stator windings, respectively; i_{ds} and i_{qs} are the stator d - and q -axis current components, respectively; i_{dr} and i_{qr} are the rotor d - and q -axis current components, respectively; ω_s is the rotational speed of the synchronous reference frame; and r_s and L_m are the stator resistance and mutual inductance, respectively. Similarly, the rotor active power is calculated by

$$P_r = \frac{3}{2} (V_{dr} i_{dr} + V_{qr} i_{qr}) \approx \frac{3}{2} [-s w_s L_m (i_{qs} i_{dr} - i_{ds} i_{qr}) + r_r (i_{dr}^2 + i_{qr}^2)] \quad (8)$$

where v_{dr} and v_{qr} are the d - and q -axis voltage components of the rotor windings, respectively; s is the slip of the DFIG defined by

$$s = (\omega_s - \omega_r) / \omega_s \quad (9)$$

where ω_r is the DFIG rotor speed. (7) and (8) yield

$$P_r = -s P_s \quad (10)$$

According to (6) and (10) $P_{si,max}$ and $P_{ri,max}$ of each WTG can be determined. Then, the total maximum mechanical power $P_{m,max}$, DFIG output active power $P_{e,max}$, and stator

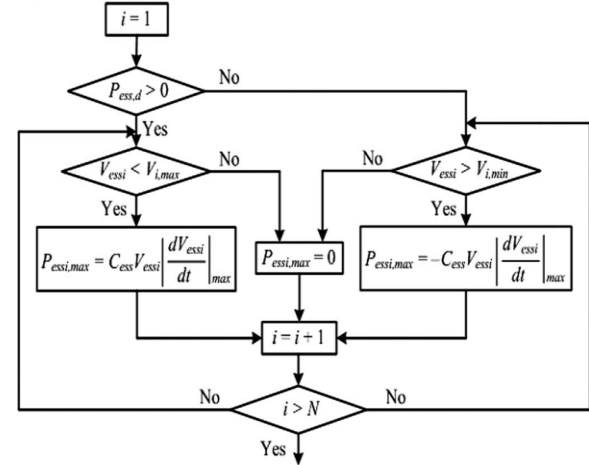


Fig.7. Flowchart of determination of $P_{ess,i,max}$ for each WTG.

active power $P_{s,max}$ of all WTGs in the wind farm can be calculated as

$$P_{m,max} = \sum_{i=1}^N P_{mi,max} \quad (12)$$

$$P_{e,max} = \sum_{i=1}^N P_{ei,max} \quad (13)$$

$$P_{s,max} = \sum_{i=1}^N P_{si,max} \quad (14)$$

In order to supply constant power P_d to the grid, the deviation $P_{ess,d}$ between the demand/commitment P_d and the maximum generation $P_{e,max}$ is the power that should be stored in or supplied from the ESSs of the WTGs

$$P_{ess,d} = P_{e,max} - P_d \quad (15)$$

On the other hand, the capability of each ESS to store or supply power depends on the capacitance C_{ess} and the voltage $V_{ess,i}$ of the supercapacitor bank. During normal operation, $V_{ess,i}$ must be maintained within the following range:

$$V_{i,min} < V_{ess,i} < -V_{i,max} \quad (16)$$

where $V_{i,max}$ and $V_{i,min}$ are the maximum and minimum operating voltages of the supercapacitor bank, respectively. The maximum power $P_{ess,i,max}$ that can be exchanged between the supercapacitor bank and the DFIG dc link of WTG i can be determined by

$$P_{ess,i,max} = \pm C_{ess} V_{ess,i} \left| \frac{dV_{ess,i}}{dt} \right|_{max} \quad (17)$$

where $|dV_{ess,i}/dt|_{max}$ is the maximum rate of voltage variations of the supercapacitor bank, which is related to the current limits of the supercapacitor bank. In (17), the positive sign indicates storing

energy, while the negative sign indicates supplying energy by the ESS. The calculation of $P_{ess,max}$ for each WTG is subjected to (16). Fig. 7 shows how to determine $P_{ess,max}$ for each WTG. If $P_{ess,d} > 0$, extra power needs to be stored in the ESSs. In this case, if $V_{ess,i} < V_{i,max}$, $P_{ess,max}$ is calculated by (17) and takes the positive sign; otherwise, the ESS cannot store any power and $P_{ess,max} = 0$. On the contrary, if $P_{ess,d} < 0$, active power needs to be supplied from the ESSs. In this case

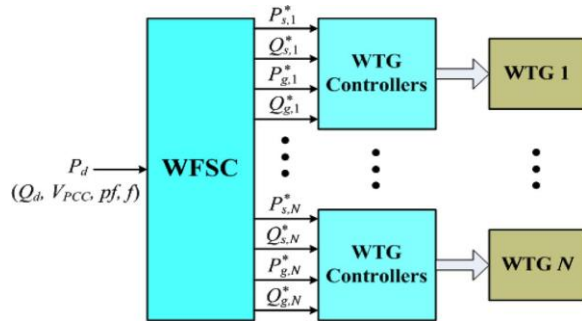


Fig.8. Proposed two-layer CPC scheme for the wind farm.

if $V_{ess,i} > V_{i,min}$, $P_{ess,max}$ is calculated by (17) and takes the negative sign; otherwise, the ESS cannot supply any power and $P_{ess,max} = 0$. As shown in Fig. 6, once $P_{ess,max}$ of each WTG is determined, the total maximum power $P_{ess,max}$ that can be exchanged between the supercapacitor bank and the DFIG dc link of all WTGs can be determined by

V. SIMULATION RESULTS

Simulation studies are carried out for a wind farm with 15 DFIG wind turbines (see Fig. 9) to verify the effectiveness of the proposed control scheme under various operating conditions. Each DFIG wind turbine (see Fig. 1) has a 3.6-MW power capacity [14], [15]. The total power capacity of the wind farm is 54 MW. Each DFIG wind turbine is connected to the internal network of the wind farm through a 4.16/34.5-kV voltage step-up transformer. The high-voltage terminals of all transformers in the wind farm are connected by 34.5-kV power cables to form the internal network of the wind farm. The entire wind farm is connected to the utility power grid through a 34.5/138-kV voltage step-up transformer at PCC to supply active and reactive powers of P and Q , respectively. In this paper, the power grid is represented by an infinite source. The ESS of each WTG is designed to continuously supply/store 20% of the DFIG rated power for approximately 60 s. Then, the total capacitance of the supercapacitor bank can be obtained from (1). The parameters of the WTG, the ESS, and the power network are listed in the Appendix. Some typical results are shown and discussed in this section.

A. CPC During Variable Wind Speed Conditions

Fig. 9 shows the wind speed profiles of WTG1 (v_{w1}), WTG6 (v_{w6}), and WTG11 (v_{w11}). The wind speeds across the three WTGs vary in a range of ± 3 m/s around their mean value of 12 m/s. The variations of wind speed cause fluctuations of the electrical quantities of the WTGs. If the wind farm is not equipped with any energy storage devices operator, where each WTG is equipped with an ESS as shown in Fig. 1. The ESS stores energy when the WTG generates more active power than the demand/commitment and supplies energy when the WTG generates less active power than the demand/commitment. The resulting output power of the wind farm is therefore controlled at a constant value as required by the grid operator.

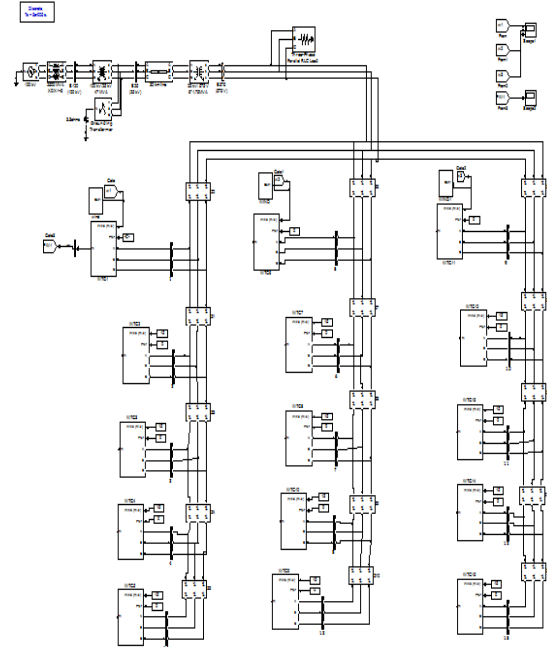


Fig. 9. Without energy storage system

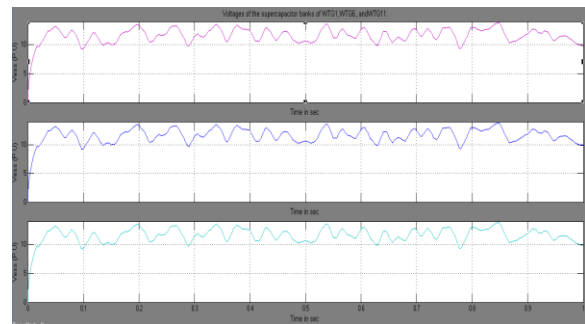


Fig. 10. Scope 1

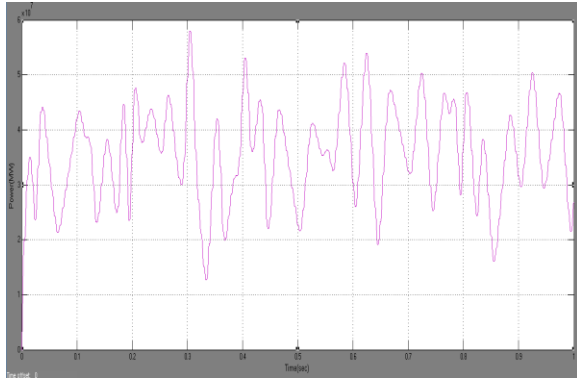


Fig. 11. Scope 2

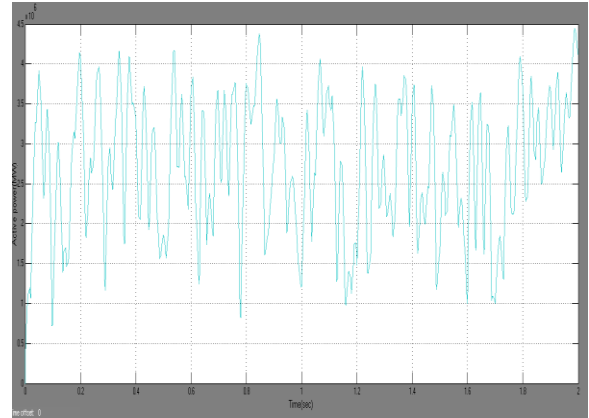


Fig.14. Scope 2

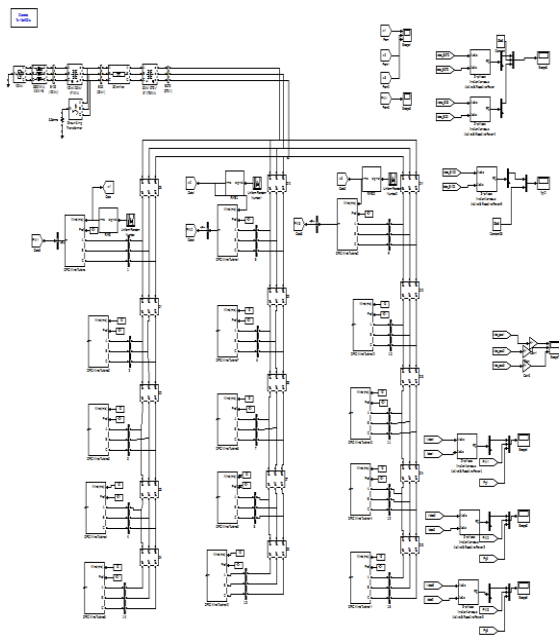


Fig.12. With energy storage system

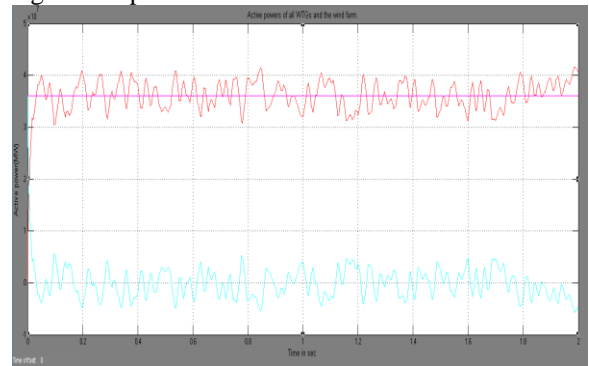


Fig.15. Scope 3

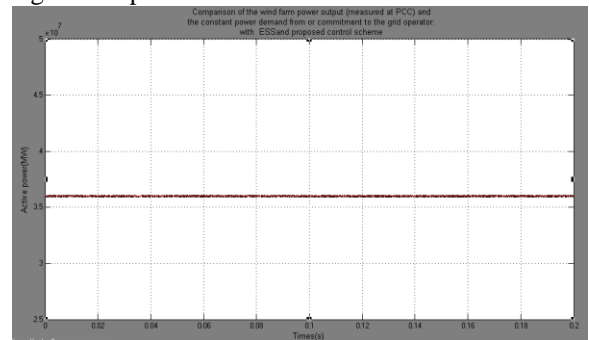


Fig.16.

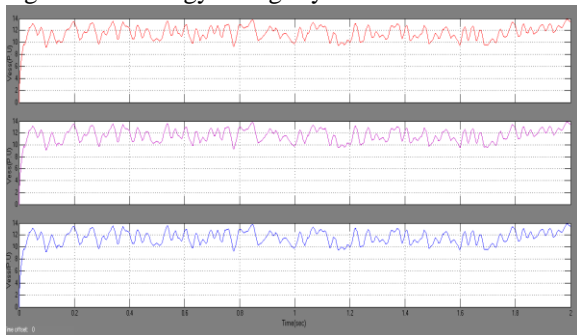


Fig.13. Scope 1

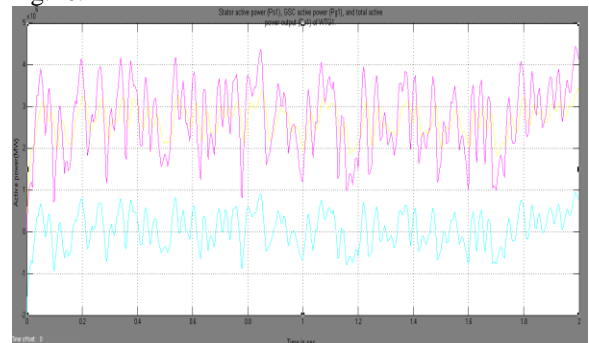


Fig.17. Scope 4

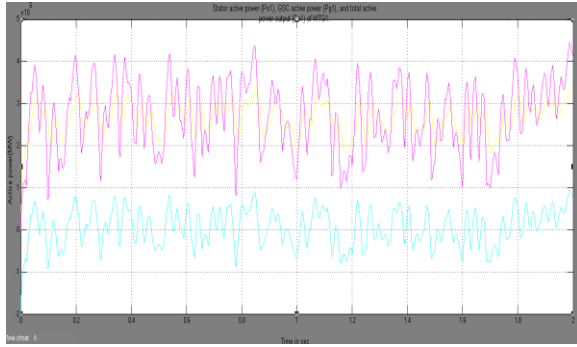


Fig.18. Scope 5

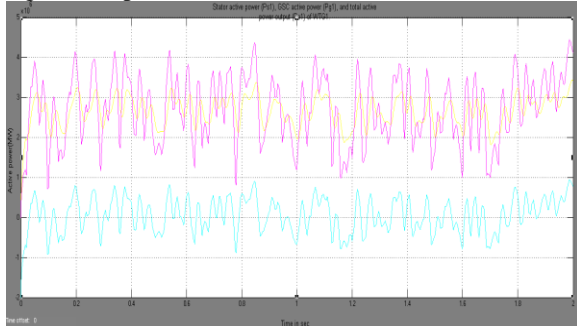


Fig.19. Scope 6

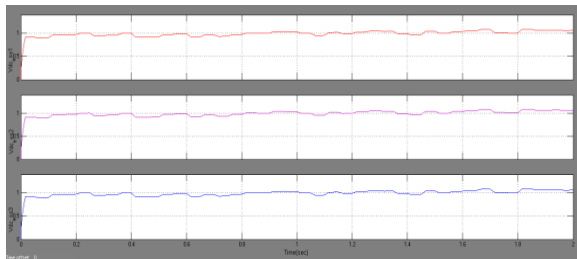


Fig.20. Scope 7

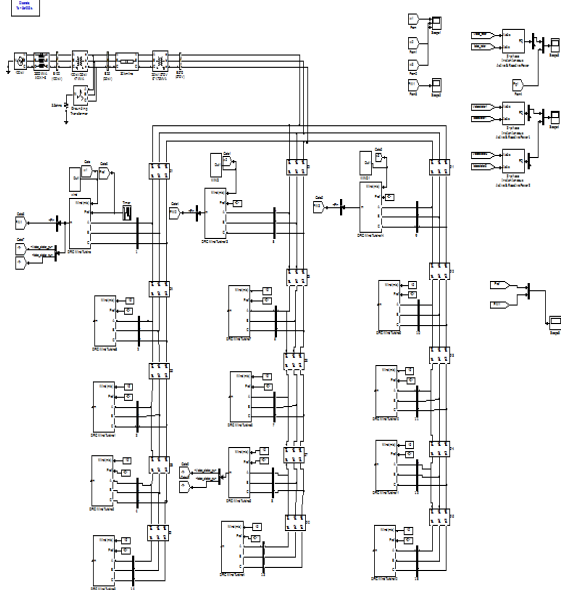


Fig.21 Power tracking during step change in demand

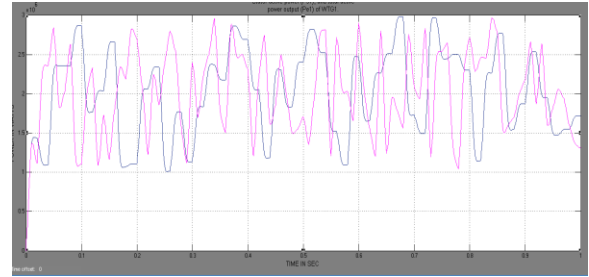


Fig.22. Scope 3

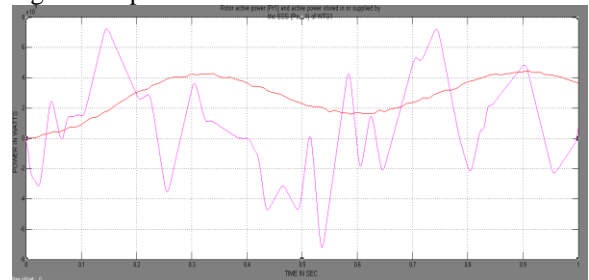


Fig.23. Scope 4

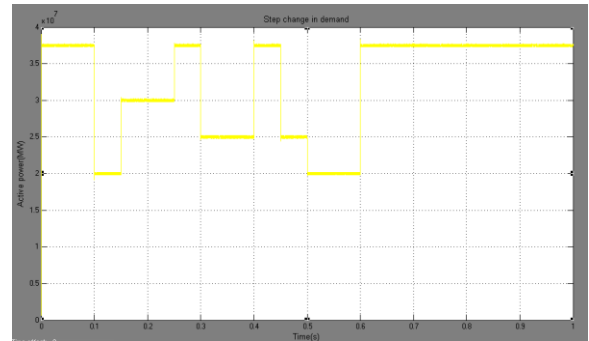


Fig.24. Scope 2

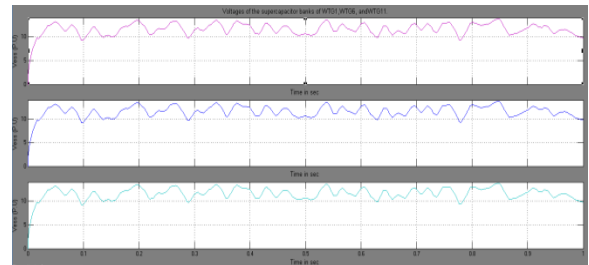


Fig.25. Scope 1

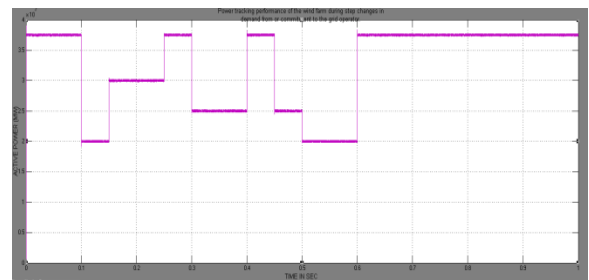


Fig.26. Scope 5

VI. CONCLUSION

This paper has proposed a novel two-layer CPC scheme for a wind farm equipped with DFIG wind turbines. Each wind turbine is equipped with a supercapacitor-based ESS, which is connected to the dc link of the DFIG through a two-quadrant dc/dc converter. The ESS serves as either a source or a sink of active power to control the generated active power of the DFIG wind turbine. Each individual DFIG wind turbine and its ESS are controlled by low-layer WTG controllers, which are coordinated by a high-layer WFSC to generate constant active power as required by or committed to the grid operator. Simulation studies have been carried out for a wind farm equipped with 15 DFIG wind turbines to verify the effectiveness of the proposed CPC scheme. Results have shown that the proposed CPC scheme enabled the wind farm to effectively participate in unit commitment and active power and frequency regulations of the grid. The proposed system and control scheme provides a solution to help achieve high levels of penetration of wind power into electric power grids.

REFERENCES

- [1] "Focus on 2030: EWEA aims for 22% of Europe's electricity by 2030," *Wind Directions*, pp. 25–34, Nov./Dec. 2006.
- [2] 20% Wind Energy By 2030: Increasing Wind Energy's Contribution to U.S. Electricity Supply, U.S. Department of Energy, Jul. 2008.
- [3] W. Qiao and R. G. Harley, "Grid connection requirements and solutions for DFIG wind turbines," in *Proc. IEEE Energy Conf.*, Atlanta, GA, Nov. 17–18, 2008, pp. 1–8.
- [4] Wind Generation & Total Load in the BPA Balancing Authority: DOE Bonneville Power Administration, U.S. Department of Energy. [Online]. Available: <http://www.transmission.bpa.gov/business/operations/Wind/default.aspx>
- [5] R. Piwko, D. Osborn, R. Gramlich, G. Jordan, D. Hawkins, and K. Porter, "Wind energy delivery issues: Transmission planning and competitive electricity market operation," *IEEE Power Energy Mag.*, vol. 3, no. 6, pp. 47–56, Nov./Dec. 2005.
- [6] L. Landberg, G. Giebel, H. A. Nielsen, T. Nielsen, and H. Madsen, "Shortterm prediction—An overview," *Wind Energy*, vol. 6, no. 3, pp. 273–280, Jul./Sep. 2003.
- [7] M. Milligan, B. Kirby, R. Gramlich, and M. Goggin, Impact of Electric Industry Structure on High Wind Penetration Potential, Nat. Renewable Energy Lab., Golden, CO, Tech. Rep. NREL/TP-

55046273.[Online]. Available: <http://www.nrel.gov/docs/fy09osti/46273.pdf>

- [8] J. P. Barton and D. G. Infield, "Energy storage and its use with intermittent renewable energy," *IEEE Trans. Energy Convers.*, vol. 19, no. 2, pp. 441–448, Jun. 2004.
- [9] D. Rastler, "Electric energy storage, an essential asset to the electric enterprise: Barriers and RD&D needs," *California Energy Commission Staff Workshop Energy Storage Technol., Policies Needed Support California's RPS Goals 2020*, Sacramento, CA, Apr. 2, 2009.
- [10] C. Abbey and G. Joos, "Supercapacitor energy storage for wind energy applications," *IEEE Trans. Ind. Appl.*, vol. 43, no. 3, pp. 769–776, May/Jun. 2007.
- [11] B. S. Borowy and Z. M. Salameh, "Dynamic response of a stand-alone wind energy conversion system with battery energy storage to wind gust," *IEEE Trans. Energy Convers.*, vol. 12, no. 1, pp. 73–78, Mar. 1997.
- [12] M.-S. Lu, C.-L. Chang, W.-J. Lee, and L. Wang, "Combining the wind power generation system with energy storage equipments," *IEEE Trans. Ind. Appl.*, vol. 45, no. 6, pp. 2109–2115, Nov./Dec. 2009.
- [13] A. Yazdani, "Islanded operation of a doubly-fed induction generator (DFIG) wind-power system with integrated energy storage," in *Proc. IEEE Canada Elect. Power Conf.*, Montreal, QC, Canada, Oct. 25–26, 2007, pp. 153–159.

AUTHOR DETAILS



V. Krishnamurthy received the B.Tech degree from St. John's College of Engineering and Technology, Yemmiganur. Affiliated to JNTU Ananthapur. Presently he is pursuing M.Tech from Narayana Engineering College, Nellore.



Ch. Rajesh Kumar received the Master degree in electrical power engineering from Anna University Chennai, B.Tech degree from Sri Vidyanikethan Engineering College. Affiliated to JNTU Ananthapur. Ragampet.

Tirupathi. Currently, He is Asst.proffesor of electrical and electronics engineering at Narayana Engineering College, Nellore,AP.